

## Phase Pattern Formation in Grain Boundaries

I. S. Winter<sup>1,\*</sup> and T. Frolov<sup>2,†</sup>

<sup>1</sup>*Sandia National Laboratories, Albuquerque, New Mexico 87123, USA*

<sup>2</sup>*Lawrence Livermore National Laboratory, Livermore, California 94550, USA*

 (Received 14 December 2023; accepted 22 March 2024; published 3 May 2024)

In this Letter we derive conditions that predict the existence of two-phase periodic-pattern grain boundary structures that are stable against coarsening. While previous research has established that elastic effects can lead to phase pattern formation on crystal surfaces, the possibility of stable grain boundary structures composed of alternating grain boundary phases has not been previously analyzed. Our theory identifies the specific combination of grain boundary and materials properties that enable the emergence of patterned grain boundary states and shows that the dislocation content of grain boundary phase junctions, absent in surface phenomena, weakens the stability of the patterned structures. The predictions of the theory are tested using a model copper grain boundary that exhibits multiple phases and two-phase pattern formation. We discuss how, similarly to surfaces, elastic effects associated with grain boundary phase junctions have profound implications for how grain boundary phases transform.

DOI: [10.1103/PhysRevLett.132.186204](https://doi.org/10.1103/PhysRevLett.132.186204)

Long-range elastic interactions are known to have profound effects on phase transformations and microstructural evolution [1], enabling phenomena such as 2D self-assembling systems [2–4], reverse coarsening [5,6], and the formation of helium bubble superlattices within a crystalline material [7]. Elastic effects arising from interactions between junctions of surface phases are known to have a profound effect on phase transformations in two dimensions [8,9]. Line forces, also known as force monopoles, exist at surface phase junctions due to the difference in surface stress [8,10–13]. A seminal study by Marchenko and Parshin showed that the interaction of these surface line defects can in some cases reduce the surface energy of the system relative to a coarse two-phase state [10]. This stabilizes a new surface structure, which can be described as a periodic pattern composed of alternating surface phases. The characteristic dimensions of the pattern depend on the temperature, composition, and elastic properties of the system.

Thermodynamics, which does not consider long-range interactions, predicts surface phase diagrams with well-defined phase equilibrium lines that correspond to the equilibrium coexistence of the different phases. In reality, elastic interactions can smear the coexistence lines defined by the equality of free energies, creating a new domain represented by the patterned state. Patterned surface states with a well-defined pattern wavelength and no well-defined transition temperature have been experimentally observed and confirmed for surface phases of silicon [9].

Grain boundaries are internal interfaces inside a material that, just like surfaces, exhibit different phases for fixed macroscopic degrees of freedom [14–16], separated by line defects called grain boundary phase junctions (GBPJs). Just

as for surfaces, the junctions between different GB phases give rise to line forces, because different GB phases have different GB stresses [17]. In this regard, GB phases are equivalent to surface phases and have the potential for forming patterned states. However, one crucial distinction is that GB phase junctions also contain dislocations [17–19]. This additional, positive, dislocation-dislocation interaction energy contribution can overcome the negative elastic energy of line forces and destabilize the patterned GB state. Recently, stable faceted grain boundaries with nanometer-sized facets, a related patterning phenomenon, have been directly observed in copper [20], confirming theoretical stability conditions proposed by Hamilton *et al.* [21]. However, the possibility of metastable pattern formation at GBs is currently not known. In this Letter, we derive equations describing the energy of the patterned states at GBs that include both line forces and dislocation interactions and demonstrate conditions under which patterned GB states can exist. Using the predictions of our model we identify a model copper GB system that exhibits pattern behavior. Our simulations demonstrate that the structure composed of alternating GB phases is stable against coarsening at finite temperatures.

In a manner analogous to Hamilton *et al.*'s study of GB facets [21], let us consider a periodic GB phase pattern consisting of two GB phases as depicted in Fig. 1. We will term the two GB phases to be the  $\alpha$  and  $\beta$  phases. The repeat distance of the pattern is of length  $d$ , and the lengths of the  $\alpha$  and  $\beta$  phases are  $l$  and  $d - l$ , respectively. Both a line force and dislocation can exist at the GB phase junction [17]. The line force arises due to the difference in GB stresses:  $\mathbf{f} = (\tau_{11}^{\alpha} - \tau_{11}^{\beta})\hat{\mathbf{e}}_1$ . The dislocation is a result of the

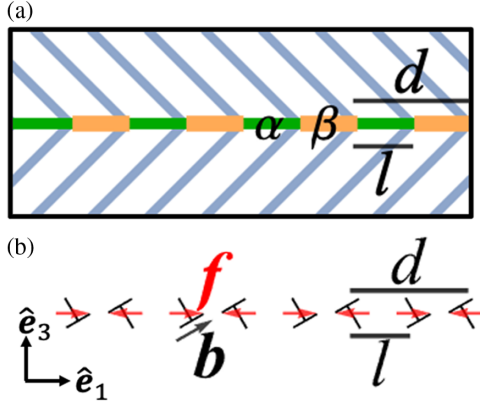


FIG. 1. Panel (a) depicts a schematic of a periodic GB phase pattern, with the  $\alpha$  and  $\beta$  GB phases represented by green and orange regions. The repeat length of the pattern is  $d$  and the length of the  $\alpha$  phase is  $l$ . Panel (b) depicts the corresponding periodic pattern of GBPJs represented as line forces and dislocations.

difference in excess volume, excess shear, and the density of atoms at the GB for the two GB phases [18]. The energy per unit area of such a two-phase pattern depicted in Fig. 1 is expressed in terms of  $\chi = l/d$  as

$$E(\chi) = \Delta\gamma^{\alpha\beta}\chi + \frac{A}{d} \ln\left(\frac{d \sin(\pi\chi)}{\pi\rho}\right) + \frac{2\Gamma^{\alpha\beta} + B}{d}, \quad (1)$$

where  $\Delta\gamma^{\alpha\beta} = \gamma^\alpha - \gamma^\beta$  is the difference in GB energy between the  $\alpha$  and  $\beta$  GB phases.  $A$  and  $B$  are elastic terms, of units energy per unit length, related to  $f$ ; the Burgers vector,  $\mathbf{b}$ ; and the elastic constants of the bulk material.  $\rho$  and  $\Gamma^{\alpha\beta}$  are the core radius and core energy per unit length of the GBPJ. A derivation of Eq. (1) is given in the Supplemental Material [22].

From Eq. (1) it can be shown that a local maximum or minimum energy exists for the dual-phase system if  $dE(\chi)/d\chi = 0$ , for some  $\chi \in (0, 1)$ . For pattern formation

to be at least metastable, this extreme point,  $\chi_c$ , must be a local minimum:  $d^2E(\chi)/d\chi^2|_{\chi=\chi_c} > 0$ . As  $d^2E(\chi)/d\chi^2 = -\pi^2 A/d\sin^2(\pi\chi)$ , the possibility for pattern formation to occur is entirely dependent on the sign of the elastic coefficient,  $A$ . If  $A < 0$ , a pattern can exist in a metastable state. The metastable patterned state containing two different GB phases is energetically stabilized against coarsening by the elastic energy of the interacting GBPJs, which is not to be confused with the mixed states stabilized by entropy discussed in Refs. [23,24].

In the general case, when using anisotropic elasticity theory, we can only compute a numerical value for  $A$ . However, to better understand the conditions necessary for pattern formation to occur, we consider the case of an elastically isotropic system, as this allows us to write a symbolic closed-form expression for  $A$  [17]:

$$A = A^{dd} + A^{pp} + A^{dp}, \quad (2a)$$

$$A^{dd} = \mu[(1-\nu)b_2^2 + (b_1^2 + b_3^2)^2]/2\pi(1-\nu), \quad (2b)$$

$$A^{pp} = -f_1^2(3-4\nu)/8\pi\mu(1-\nu), \quad (2c)$$

$$A^{dp} = -f_1 b_3(1-2\nu)/2\pi(1-\nu), \quad (2d)$$

where  $\mu$  is the shear modulus,  $\nu$  Poisson's ratio and  $b_i$  the components of the Burgers vector. The first term in  $A$ , the elastic coefficient related to the dislocation-dislocation interaction,  $A^{dd}$ , must be positive if the material is to be elastically stable. The second term,  $A^{pp}$ , the line force-line force interaction must be negative if the material is to be elastically stable.  $A^{dp}$ , the line force-dislocation interaction can be positive or negative depending on the signs of  $f_1$  and  $b_3$ .

Let us now try to find what values of  $f_1$  allow for  $A < 0$ .  $A$  is a quadratic equation with respect to  $f_1$ , so finding the roots of  $f_1$  is instructive:

$$f_1^{0,\text{low}} = -\frac{2\mu}{3-4\nu} \left( b_3(1-2\nu) + \sqrt{b_1^2(3-4\nu) + (1-\nu)[4b_3^2(1-\nu) + b_2^2(3-4\nu)]} \right), \quad (3a)$$

$$f_1^{0,\text{high}} = -\frac{2\mu}{3-4\nu} \left( b_3(1-2\nu) - \sqrt{b_1^2(3-4\nu) + (1-\nu)[4b_3^2(1-\nu) + b_2^2(3-4\nu)]} \right). \quad (3b)$$

Mechanical stability requires that  $-1 < \nu < 1/2$ , so the roots of  $f_1$  must be real for an elastically stable material. A necessary condition for pattern formation,  $A < 0$ , is met if  $f_1 > f_1^{0,\text{high}}$  or  $f_1 < f_1^{0,\text{low}}$ . Thus the theory allows us to formulate the following screening criteria for GBs capable of pattern formation. GB phases should have large differences in GB stresses, a small Burgers vector at the GBPJ, and a small shear modulus of the material.

Following the criteria identified by the theory we consider the possibility of pattern formation in a face-centered-cubic Cu  $\Sigma 5(210)[001]$  GB composed of repeating units of split-kite and filled-kite GB phases [25]. These two GB phases have a large difference in  $\tau_{11}$  as shown in Table I resulting in a large line force,  $f_1 = -4.66 \text{ J/m}^2$ , while the Burgers content is relatively small,  $b < 0.5 \text{ \AA}$  [18]. In this reference frame, the  $\hat{e}_1$  direction corresponds to

TABLE I. Properties of the two grain boundary phases considered in this Letter.

GB phase	Split kite	Filled kite
GB energy (J/m <sup>2</sup> )	0.942	0.953
$\tau_{11}$ (J/m <sup>2</sup> )	-2.36	2.30
Structural unit area ( $a_0^2$ )	$\sqrt{5} \times 2$	$2\sqrt{5} \times 7$
Fraction of plane	1/2	6/7

$\langle 210 \rangle$  and the  $\hat{e}_2$  direction corresponds to  $\langle 001 \rangle$ . To match the boundary dimensions along the tilt axis in our co-existence simulations we selected metastable, but near to the ground state, split- and filled-kite structures [26].

Following the work of Barnett and Lothe [27], we applied anisotropic linear elasticity theory to calculate the elastic coefficient in Eq. (1),  $A$ , using an embedded-atom method potential of Cu [28] within the molecular dynamics simulation code, LAMMPS [29]. Equation (1) remains valid in the anisotropic case, but in general the elastic coefficient  $A$  can only be determined numerically [27]. At 0 K,  $A$  was calculated from the elastic constants of the system,  $\tau_{11}$  for each GB phase (given in Table I), and the Burgers vector of the GBPJ. Using the approach outlined in Ref. [18], we found the Burgers vector of the GBPJ to be  $\mathbf{b} = -0.368\hat{e}_3$ . From these inputs we find  $A = -31 \text{ meV}/\text{\AA}$ , and as a result, predict pattern formation to occur.

To test if the magnitude of  $A$  is large enough to maintain pattern stability in the presence of thermal fluctuations, we first consider 0 K molecular statics simulations of the effect of pattern morphology on system energy. Since the two different grain boundary phases are composed of a different number of atoms (Table I) and the total number of atoms in the simulation box is fixed, a heterogeneous state composed of just two GB phase islands is always stable in a finite temperature interval [30]. As a result, to investigate the stability against coarsening, we have to consider a double-period system consisting of four GB phases repeating over a length  $D$ , two split kites, and two filled kites as shown in Fig. 2(a). The double-period system is constructed such that the total length of split- and filled-kite islands is constant, and as a result the number of atoms in the system too: if one split-kite island grows in length, the other shrinks. If we constrain the larger (smaller) split-kite island to have the same length as the larger (smaller) filled-kite island, we can describe the system with one parameter,  $\Delta l$ : the difference in length between the two islands of a given GB phase junction, shown in Fig. 2. The elastic energy from such a double-period structure can be written as

$$\Delta E^{DP}(\Delta l) = A \ln \left( \cos \left( \frac{2\pi\Delta l}{D} \right) \right). \quad (4)$$

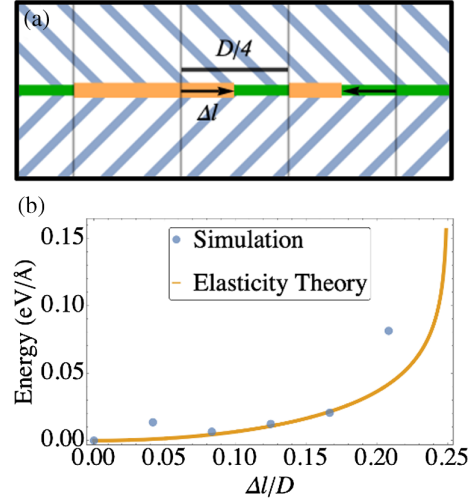


FIG. 2. Panel (a) depicts the double-period GB-phase-patterned state. Panel (b) shows a comparison of the energy of a double-period structure using molecular statics simulations and elasticity theory. The increasing energy shows that the patterned state is stable against coarsening.

The derivation of Eq. (4) is detailed in the Supplemental Material [22]. In Fig. 2, Eq. (4) is compared to molecular statics simulations of the double-period system as a function of  $\Delta l$ , which are generated using the method described in Ref. [17]. As the simulations contained approximately 500 000 atoms, the molecular statics simulations of the double-period structure were performed by annealing the structures at 300 K for 20 ns and then relaxing the structure using the FIRE optimization algorithm [31]. While the grain boundary structures were already in their lowest energy states from the beginning, the structure of the GBPJ cores required additional optimization which occurred during the annealing stage. The GB energy of all systems converged to  $10^{-8} \text{ eV}/\text{\AA}^2$ . However, due to the large system size and complex GB microstructure, the scatter of the 0 K energies is still seen in Fig. 2. Overall, however, we see an excellent agreement between the prediction of Eq. (4) and direct GB energy calculations of the patterned state using molecular statics at 0 K. Both calculations suggest that the regular patterned state should be stable against coarsening.

To investigate the effect of temperature on the stability of the patterned state, we calculated  $A$  in the temperature interval from 0 to 1000 K ( $\approx 0.75T_m$ ). We note that the melting point,  $T_m$ , of this potential is found to be 1327 K [32]. This required the calculation of the elastic constants,  $\tau_{11}$ , and thermal expansion as a function of temperature, the details of which are given in the Supplemental Material [22]. The calculated elastic coefficient  $A(T)$  is shown in Fig. 3. It remains negative, predicting the stability of the patterned state at finite temperature. The temperature however has a destabilizing effect as  $A$  gradually decreases

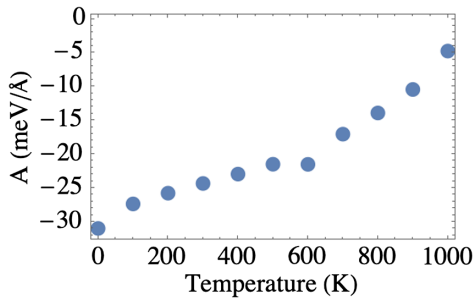


FIG. 3. The elastic coefficient  $A$ , plotted as a function of temperature confirms the stability of the patterned state at finite temperatures. Its decreasing magnitude suggests that the temperature decreases the stability of the patterned state. Error bars are smaller than the size of the data points.

in magnitude and reaches a near zero value at 1000 K, marking the limit of the patterned state’s stability.

Finally, we tested the predictions of our theory and calculations by directly simulating the evolution of the double-period patterned state at high temperature using molecular dynamics in the NVT ensemble. The patterned state containing four GB phase islands shown in Fig. 4 should be stable against coarsening into a two-phase state. For our MD simulations, we selected 800 K as the optimal testing temperature. At higher temperatures, the stabilizing force becomes vanishingly small and comparable to fluctuations, so we expect the pattern to go away. At lower temperatures, the island size fluctuations become too

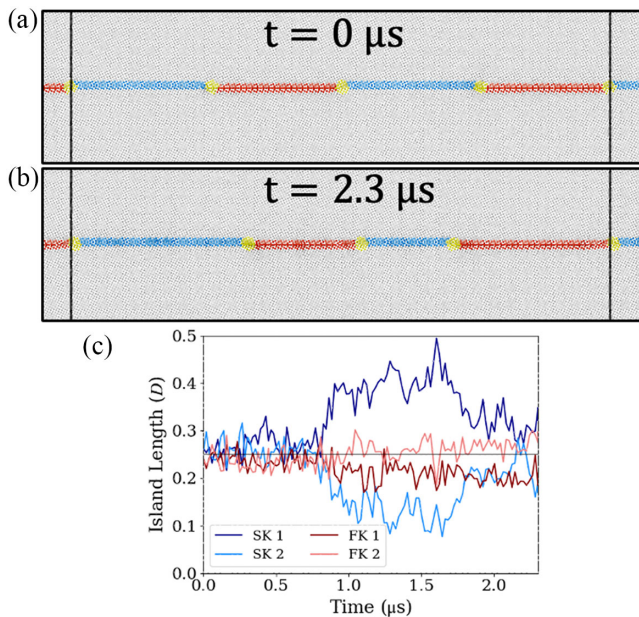


FIG. 4. Panels (a) and (b) depict the initial and final island configurations. Blue atoms correspond to split-kite islands, red atoms correspond to filled-kite islands, and yellow atoms correspond to GB phase junctions. Panel (c) shows the evolution of islands over time.

infrequent to provide convincing proof of stability. The initial patterned state with all four islands of equal length,  $l = D/4$ , is shown in Fig. 4(a). We ran the simulation for a total of 2.3  $\mu\text{s}$ .

We estimated the lengths of the four islands, shown in Fig. 4(c), by calculating the contour of the GB (and the step heights between GB phase junctions). The contour was estimated by applying polyhedral template matching [33], as implemented in OVITO [34], with non-FCC atoms considered to be part of the GB. Hyperbolic tangent functions were fit to the GB contour to calculate island lengths, with more details of the simulation given in the Supplemental Material [22]. The GB pattern showed remarkable stability during the first 0.75  $\mu\text{s}$ , during which the length of all islands fluctuated around the equal size state with  $l = D/4$ , as shown in Fig. 4(c). We note that states with different  $l$  are visited during this time interval as the junctions migrate by several GB units (see movie in the Supplemental Material [22]).

At approximately  $t = 0.75 \mu\text{s}$  we observe a large fluctuation towards a coarser state when the length of one of the split-kite islands increases significantly at the expense of the other split-kite island. However, at approximately 1.75  $\mu\text{s}$ , the system returns to the patterned state, confirming its stability. The state of the system after 2.3  $\mu\text{s}$  is shown in Fig. 4(b).

The observed large fluctuation of the island size away from the even size state at 800 K is indicative of an already very small stabilizing contribution from the elastic interactions compared to thermal fluctuations. We expect that at higher temperatures thermal fluctuations will dominate the evolution of such a microstructure eventually leading to coarsening. At lower temperatures on the other hand we expect the patterned state to be stable.

There is an increasing recognition that just like in 3D materials, complex defect microstructures exist inside interfaces and greatly influence the properties of polycrystalline materials. GBs may contain ordered or random networks of disconnections and/or GB phase junctions. These defected GB microstructures could form during nonequilibrium processes such as plastic deformation, grain growth, exposure to fluxes of point defects during radiation damage, and other processes that involve changes in temperature and chemical composition.

Our understanding of the dynamic evolution and stability of these GB defect microstructures is currently severely limited by the lack of techniques that enable the identification and visualization of these defects in the GB plane both experimentally and in simulations. Only recently, algorithms capable of robust identification of disconnection and GB phase junctions have been proposed [19,35]. Despite these limitations, there is growing interest in understanding the collective behavior of disconnections and GB phase junctions. For example, a recent theoretical study predicted GB topological transitions due to disconnections

[36], which could result in dramatic changes in GB mobility [37].

The GB patterns studied in this Letter effectively introduce a stable uniformly spaced network of disconnections (GBPJs) on the GB plane and could have beneficial properties with respect to radiation damage. Each of these junctions is a near-ideal source or sink of atoms, because when such a junction moves, atoms are absorbed or released due to the GB transformation. Such a network of disconnections (GBPJs) could also have a beneficial impact on mechanical properties such as ductility by providing dislocation nucleation sites on the GB.

Complex dual-phase patterns composed of different GB phases have recently been investigated by high-resolution transmission electron microscopy (HRTEM) in Cu GBs [38,39], with dual-phase patterned GB microstructures having been directly observed by HRTEM in  $\langle 111 \rangle$  tilt GBs in Cu [39]. To explain the pattern metastability the authors of the study postulated that an array of preexisting disconnections inherited from processing could exist at the boundary and these disconnections would effectively repel GB phase junctions and make this dual-phase patterned structure metastable. Using our analysis, we can estimate the elastic coefficient to be  $A = 40 \text{ meV}/\text{\AA}$ , which means that this particular Cu GB (without additional preexisting disconnections) should not form a metastable patterned state. We conclude that the observed state is either a result of an incomplete transformation or indeed the presence of a preexisting array of additional disconnections.

Inspired by well-known theoretical and experimental results for surface phases, here we investigated the stability of patterned states of GBs composed of different GB phases separated by line defects containing both line forces and dislocations. We derived equations describing the energy of such states and identified conditions where the patterned state becomes metastable, providing a barrier to coarsening into a more common two-phase structure. We show that the Burgers content present at GB phase junctions has a destabilizing effect on the patterned state. Using our theoretical model we identified a model system that should exhibit pattern behavior and verified it by direct atomistic simulations at finite temperature as well as energy calculations at 0 K.

This work was performed under the auspices of the U.S. Department of Energy (DOE) by Lawrence Livermore National Laboratory under Contract No. DE-AC52-07NA27344. T.F. was supported by the U.S. DOE, Office of Science under an Office of Fusion Energy Sciences Early Career Award. Computing support for this work came from the Lawrence Livermore National Laboratory Institutional Computing Grand Challenge program. Sandia National Laboratories is a multi-mission laboratory managed and operated by National Technology & Engineering Solutions of Sandia, LLC

(NTESS), a wholly owned subsidiary of Honeywell International Inc., for the U.S. Department of Energy's National Nuclear Security Administration (DOE/NNSA) under Contract No. DE-NA0003525. T.F. is grateful to Mark Asta for stimulating discussions.

\*iswinte@sandia.gov

†frolov2@llnl.gov

- [1] A. G. Khachaturyan, *Theory of Structural Transformations in Solids* (Dover Publications, Mineola, New York, 2008).
- [2] N. V. Medhekar, V. B. Shenoy, J. B. Hannon, and R. M. Tromp, *Phys. Rev. Lett.* **99**, 156102 (2007).
- [3] P. Müller and A. Saúl, *Surf. Sci. Rep.* **54**, 157 (2004).
- [4] S. Rousset, V. Repain, G. Baudot, H. Ellmer, Y. Garreau, V. Etgens, J. Berroir, B. Croset, M. Sotto, P. Zeppenfeld, J. Ferré, J. Jamet, C. Chappert, and J. Lecoecur, *Mater. Sci. Eng.* **96**, 169 (2002).
- [5] Y. Wang, L.-Q. Chen, and A. G. Khachaturyan, *Phys. Rev. B* **46**, 11194 (1992).
- [6] W. Johnson, T. Abinandanan, and P. Voorhees, *Acta Metall. Mater.* **38**, 1349 (1990).
- [7] P. Johnson, A. Malcolm, and D. Mazey, *Nature (London)* **329**, 316 (1987).
- [8] V. Marchenko, *JETP Lett.* **33** (1981).
- [9] J. B. Hannon, F. J. Meyer zu Heringdorf, J. Tersoff, and R. M. Tromp, *Phys. Rev. Lett.* **86**, 4871 (2001).
- [10] V. Marchenko and A. Y. Parshin, *Sov. Phys. JETP* **52**, 129 (1980).
- [11] O. L. Alerhand, D. Vanderbilt, R. D. Meade, and J. D. Joannopoulos, *Phys. Rev. Lett.* **61**, 1973 (1988).
- [12] E. Pehlke and J. Tersoff, *Phys. Rev. Lett.* **67**, 465 (1991).
- [13] D. Srolovitz and J. Hirth, *Surface Sci.* **255**, 111 (1991).
- [14] P. R. Cantwell, M. Tang, S. J. Dillon, J. Luo, G. S. Rohrer, and M. P. Harmer, *Acta Mater.* **62**, 1 (2014).
- [15] A. R. Krause, P. R. Cantwell, C. J. Marvel, C. Compson, J. M. Rickman, and M. P. Harmer, *J. Am. Ceram. Soc.* **102**, 778 (2019).
- [16] P. R. Cantwell, T. Frolov, T. J. Rupert, A. R. Krause, C. J. Marvel, G. S. Rohrer, J. M. Rickman, and M. P. Harmer, *Annu. Rev. Mater. Res.* **50**, 465 (2020).
- [17] I. S. Winter, R. E. Rudd, T. Ooppelstrup, and T. Frolov, *Phys. Rev. Lett.* **128**, 035701 (2022).
- [18] T. Frolov, D. L. Medlin, and M. Asta, *Phys. Rev. B* **103**, 184108 (2021).
- [19] I. Winter, T. Ooppelstrup, T. Frolov, and R. Rudd, *Acta Mater.* **237**, 118067 (2022).
- [20] T. Brink, L. Langenohl, S. Pemma, C. H. Liebscher, and G. Dehm, *arXiv:2309.07595*.
- [21] J. C. Hamilton, D. J. Siegel, I. Daruka, and F. Léonard, *Phys. Rev. Lett.* **90**, 246102 (2003).
- [22] See Supplemental Material at <http://link.aps.org/supplemental/10.1103/PhysRevLett.132.186204> for derivations of the equations used in the Letter along with additional computational details.
- [23] J. Han, V. Vitek, and D. J. Srolovitz, *Acta Mater.* **104**, 259 (2016).
- [24] R. G. Hoagland and R. J. Kurtz, *Philos. Mag. A* **82**, 1073 (2002).

- [25] T. Frolov, D. L. Olmsted, M. Asta, and Y. Mishin, *Nat. Commun.* **4**, 1899 (2013).
- [26] Q. Zhu, A. Samanta, B. Li, R. E. Rudd, and T. Frolov, *Nat. Commun.* **9**, 467 (2018).
- [27] D. M. Barnett and J. Lothe, *J. Phys. F* **4**, 1618 (1974).
- [28] Y. Mishin, M. J. Mehl, D. A. Papaconstantopoulos, A. F. Voter, and J. D. Kress, *Phys. Rev. B* **63**, 224106 (2001).
- [29] A. P. Thompson, H. M. Aktulga, R. Berger, D. S. Bolintineanu, W. M. Brown, P. S. Crozier, P. J. in 't Veld, A. Kohlmeyer, S. G. Moore, T. D. Nguyen, R. Shan, M. J. Stevens, J. Tranchida, C. Trott, and S. J. Plimpton, *Comput. Phys. Commun.* **271**, 108171 (2022).
- [30] T. Frolov, W. Setyawan, R. Kurtz, J. Marian, A. R. Oganov, R. E. Rudd, and Q. Zhu, *Nanoscale* **10**, 8253 (2018).
- [31] E. Bitzek, P. Koskinen, F. Gähler, M. Moseler, and P. Gumbsch, *Phys. Rev. Lett.* **97**, 170201 (2006).
- [32] T. Frolov and Y. Mishin, *Phys. Rev. B* **79**, 045430 (2009).
- [33] P. M. Larsen, S. Schmidt, and J. Schiøtz, *Model. Simul. Mater. Sci. Eng.* **24**, 055007 (2016).
- [34] A. Stukowski, *Modelling Simul. Mater. Sci. Eng.* **18**, 015012 (2010).
- [35] N. Deka, A. Stukowski, and R. B. Sills, *Acta Mater.* **256**, 119096 (2023).
- [36] K. Chen, D. J. Srolovitz, and J. Han, *Proc. Natl. Acad. Sci. U.S.A.* **117**, 33077 (2020).
- [37] D. L. Olmsted, S. M. Foiles, and E. A. Holm, *Scr. Mater.* **57**, 1161 (2007).
- [38] T. Meiners, T. Frolov, R. E. Rudd, G. Dehm, and C. H. Liebscher, *Nature (London)* **579**, 375 (2020).
- [39] L. Langenohl, T. Brink, R. Freitas, T. Frolov, G. Dehm, and C. H. Liebscher, *Nat. Commun.* **13**, 3331 (2022).